Pramana – J. Phys. (2018) 91:5
https://doi.org/10.1007/s12043-018-1578-1

All possible tripartitions of ^{236}U isotope in collinear configuration

K P SANTHOSH*, SREEJITH KRISHNAN and JAYESH GEORGE JOSEPH

School of Pure and Applied Physics, Kannur University, Swami Anandatheertha Campus, Payyanur 670 327, India
*Corresponding author. E-mail: drkpsanthosh@gmail.com

MS received 14 August 2017; revised 13 December 2017; accepted 2 January 2018; published online 31 May 2018

Abstract. Using the recently proposed unified ternary fission model (UTFM), the tripartition of ^{236}U isotope was studied for all possible fragmentations, in which the interacting potential barrier is taken as the sum of the Coulomb and proximity potentials with fragments in collinear configuration. The highest yield is obtained for the fragmentation ^{48}Ca+^{58}Ti+^{130}Sn and next highest yield is found for ^{58}Cr+^{46}Ar+^{132}Sn, which stress the importance of doubly magic or near doubly magic nuclei in the tripartition of ^{236}U isotope. The formation of ^{68}Ni and ^{70}Ni as the edge fragments linking the doubly magic nucleus ^{132}Sn by the isotope of Si is in good agreement with experimental and theoretical studies, in the collinear cluster tripartition of ^{236}U isotope which reveals the reliability of our model (UTFM) in ternary fission.

Keywords. Spontaneous fission; ternary fission; heavy particle decay.

PACS Nos **25.85.Ca; 23.70.+j; 27.90.+b**

1. Introduction

The ternary fission is a rare process in which three charged particles are emitted from the breakup of a radioactive nucleus and in 1941, Present [1] proposed that the tripartition of uranium isotope would release 20 MeV more energy compared to the binary fission. The experimental observation of ternary fission was found for the first time by Alvarez *et al* [2] in the case of ^{235}U isotope with α-particle emitted in a direction perpendicular to the main fission fragments. Usually, ternary fission process occurs with the equatorial and collinear configurations, in which the light fragment emitted in a direction perpendicular to the main fission fragments belongs to the equatorial configuration and for the collinear configuration, the particles are emitted along the direction of the main fission fragments. In ternary fission, the three fragments are born almost simultaneously or roughly at the same time, but a sequential decay mechanism is also found in which the fissioning nuclei break into a heavy fragment and an intermediate fragment as the first step and in the next step the intermediate fragment decays into a light fragment and a ternary particle. Several theoretical models were performed to study the fragmentation of a ternary system, but a well-defined theory that includes all the important aspects of ternary fission process has however yet to be formulated. Hence, the study on ternary fission has been an interesting area for both the experimentalists and theoreticians for the last few decades [3–8].

Sometimes, the splitting of heavy radioactive nuclei takes place with three fission fragments of comparable masses and such process can be referred to as the true ternary fission. The true ternary fission processes are found to very rarely occur compared to the binary fission and observed once in every million fission events [9]. The amount of energy released in a reaction in the ternary splitting of nearly equal sized fragments was calculated by Poenaru *et al* [10,11] and it is concluded that true ternary fission process can be observed only with the assistance of highly sensitive experimental set-up. Zagrebaev *et al* [12] studied true ternary fission in the case of superheavy nuclei and found that the phenomenon of true ternary fission is due to the strong shell effects leading to a three-cluster configuration with two doubly magic tin-like cores. Vijayaraghavan *et al* [13–15] studied the true ternary fission of ^{252}Cf isotope using the three-cluster model (TCM) [16–20] proposed by Manimaran and Balasubramaniam. They came to the point that the formation of light fragment between the other two heavy fragments are expected to have the highest probability in a true ternary fission. Tashkhodjaev *et al* [21] studied true ternary fission as a sequential

mechanism in which the middle cluster was formed within a very short time, between the ruptures of two necks formed in the collinear trinuclear system. In the sequential ternary fission of ^{252}Cf isotope, they obtained a probability of 10^{-3} per binary fission event for heavy clusters like ^{70}Ni, $^{80-82}$Ge, ^{86}Se and ^{94}Kr which were formed with the clusters having mass numbers 132–140.

A new decay channel was found by Pyatkov and collaborators [22–27] for the spontaneous ternary fission of Cf and U isotopes, where the fission fragments fly apart almost collinearly and as the fission fragments break up in collinear configuration, Pyatkov and collaborators named it as collinear cluster tripartition (CCT). Also the experimental results show that the true ternary fission of heavy nuclei is possible only in collinear configuration, which is due to the low kinetic energy of the middle fragment. In the case of ^{252}Cf and ^{236}U isotopes, Nasirov *et al* [28,29] and Oertzen *et al* [30–32] studied the collinear cluster tripartition by analysing the landscape of the potential energy surfaces. The minima were obtained for the isotopes of Ca, Fe, Ge and Se with magic proton or neutron numbers. Also, the authors found that for the ^{236}U isotope, the experimentally observed ^{68}Ni was formed as the edge fragment with Sn and Si as the other two fission fragments in the ternary system, whereas ^{68}Ni was formed as the edge fragment with Sn and Ca for ^{252}Cf isotope.

Using UTFM, we have done many theoretical calculations and predictions in various isotopes of Cm, Pu and Cf isotopes [33–38]. By taking interacting barrier as the sum of Coulomb and proximity potentials, the relative yield is calculated and hence the most favourable fragment combination is obtained in the ternary fission of various isotopes of Cm, Cf and Pu with ^{4}He as the light charged particle. In the present work, the ternary fission of ^{236}U isotope is studied in detail for all possible fragmentations assuming that the fragments are formed in collinear configuration because, for heavier middle fragment (like ^{34}Si, ^{48}Ca, ^{50}Ca etc.) formed in the ternary fission process, the collinear configuration is the most preferred compared to the equatorial configuration.

The formalism used for our calculation is described in §2. The results and discussion on the tripartition or ternary fission of ^{236}U isotope in collinear configuration is given in §3 and we summarise the entire work in §4.

2. Unified ternary fission model (UTFM)

The process of ternary fission is energetically possible only if Q value of the reaction is positive, i.e.,

$$Q = M - \sum_{i=1}^{3} m_i > 0. \tag{1}$$

The mass excess values are taken from the mass tables of Wang *et al* [39] and for the isotopes for which the mass excess values are not available in ref. [39], we have taken the values from the mass tables of Moller *et al* [40]. Here, M is the mass excess of the parent and m_i is the mass excess of the fragments. The interacting potential barrier for a parent nucleus exhibiting cold ternary fission consists of Coulomb potential and nuclear proximity potential of Blocki *et al* [41,42].

The interacting potential barrier is given by

$$V = \sum_{i=1}^{3} \sum_{j>i}^{3} (V_{Cij} + V_{Pij}) \tag{2}$$

with

$$V_{Cij} = \frac{Z_i Z_j e^2}{r_{ij}}$$

as the Coulomb interaction between the fragments. Here Z_i and Z_j are the atomic numbers of the fragments and r_{ij} is the distance between the fragment centres. The nuclear proximity potential [41] between the fragments is

$$V_{Pij}(z) = 4\pi\gamma b \left[\frac{C_i C_j}{C_i + C_j}\right] \Phi\left(\frac{z}{b}\right). \tag{3}$$

Here Φ is the universal proximity potential and z is the distance between the near surfaces of the fragments. For collinear configuration, the distance of separation between the near surfaces of the fragments are $z_{12} = z_{23} = z$ and $z_{13} = 2(C_2 + z)$. In collinear configuration, the second fragment is considered to lie between the first and third fragments. The Süssmann central radii C_i of the fragments related to sharp radii R_i is

$$C_i = R_i - \left(\frac{b^2}{R_i}\right). \tag{4}$$

For R_i we use semiempirical formula in terms of mass number A_i as [41]

$$R_i = 1.28A_i^{1/3} - 0.76 + 0.8A_i^{-1/3}, \quad (i = 1, 2, 3). \tag{5}$$

The nuclear surface tension coefficient called Lysekil mass formula [43] is

$$\gamma = 0.9517[1 - 1.7826(N - Z)^2/A^2] \text{ MeV/fm}^2, \tag{6}$$

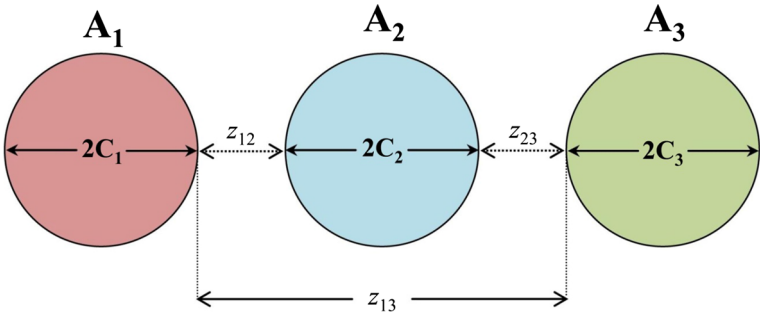

Figure 1. Schematic diagram representing three spherical fragments in collinear configuration.

where N, Z and A represent neutron, proton and mass number of the parent. Φ, the universal proximity potential, is given as

$$\Phi(\varepsilon) = -4.41\mathrm{e}^{-\varepsilon/0.7176}, \text{ for } \varepsilon > 1.9475 \quad (7)$$

$$\Phi(\varepsilon) = -1.7817 + 0.9270\varepsilon + 0.0169\varepsilon^2 - 0.05148\varepsilon^3, \quad \text{for } 0 \le \varepsilon \le 1.9475 \quad (8)$$

with $\varepsilon = z/b$, where the width (diffuseness) of the nuclear surface $b \approx 1$ Fermi.

Using one-dimensional WKB approximation, barrier penetrability P, the probability which the ternary fragments cross the three-body potential barrier, is given as

$$P = \exp\left\{-\frac{2}{\hbar}\int_{z_1}^{z_2}\sqrt{2\mu(V-Q)}\mathrm{d}z\right\}. \quad (9)$$

The first turning point $z_1 = 0$ represents touching configuration and the second turning point z_2 is determined from the equation $V(z_2) = Q$, where Q is the decay energy. The potential V in eq. (9), which is the sum of the Coulomb and proximity potentials given by eq. (2), are computed by varying the distance between the near surfaces of the fragments. The distance of separation between the surfaces of the fragments are $z_{12} = z_{23} = z$ and $z_{13} = 2(C_2 + z)$. Figure 1 represents the collinear configuration of three spherical fragments. In eq. (9) the mass parameter is replaced by the reduced mass μ and is defined as

$$\mu = m\left(\frac{\mu_{12}A_3}{\mu_{12}+A_3}\right) \quad (10)$$

and

$$\mu_{12} = m\frac{A_1A_2}{A_1+A_2}, \quad (11)$$

where m is the nucleon mass and A_1, A_2 and A_3 are the mass numbers of the three fragments.

The relative yield can be calculated as the ratio of the barrier penetrability obtained for a given fragmentation to the sum of the barrier penetrability obtained for all possible fragmentations as follows:

$$Y(A_i, Z_i) = \frac{P(A_i, Z_i)}{\sum P(A_i, Z_i)}. \quad (12)$$

Here $P(A_i, Z_i)$ represents the penetration probability for a given fragmentation in a ternary fission process. Here (A_i, Z_i) is the charge-minimised fragment combinations, where A_i denotes $A_1 + A_2 + A_3$ and Z_i denotes $Z_1 + Z_2 + Z_3$ respectively.

3. Results and discussion

We have studied the ternary fission of ^{236}U isotope taking scattering potential as the sum of Coulomb and proximity potentials, with fragments in collinear configuration. Figure 1 represents the schematic diagram of the collinear configuration of three spherical fragments. Here, fragment A_2 lies between the other two fission fragments A_1 and A_3. In this paper, we have considered all possible ternary fragmentations of ^{236}U isotope, in order to find the fragment combination with higher yields. We have studied the tripartition of ^{236}U isotope keeping the mass of the middle fragment fixed which ranges from $A_2 = 1$ to 78. When $A_2 = 1$, one possible combination is that in which the other two fragments have mass number either 117 or 118. When $A_2 = 78$, the other two fission fragments have mass numbers 79 each, which is the case of a true ternary fission. For a given value of A_2, there are various Z_2 values and hence we have considered all possible Z_2 values for a particular value of A_2. Also for a given middle fragment (A_2, Z_2) we have considered all possible mass splittings and we would like to mention that in the tripartition of ^{236}U isotope, there are about 7.786×10^5 possible ways of splitting and this value is according to the recent mass tables of Wang *et al* [39]. In the present work, we have studied all these possible fragmentations, in order to find the most probable ternary splitting of ^{236}U isotope and the repetition of the fragment combinations is avoided.

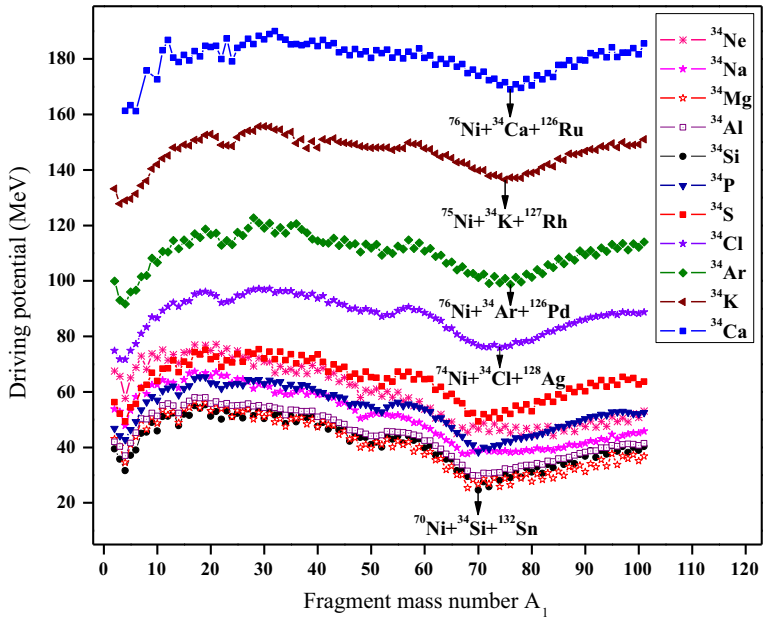

Figure 2. The driving potential plotted as a function of fragment mass number A_1 for all possible middle fragments with mass number $A_2 = 34$.

For a given middle fragment (A_2, Z_2), we have considered all possible mass splittings, using the concept of cold reaction valley which was introduced in relation to the structure of minima in the so-called driving potential. The quantum mechanical fragmentation theory (QMFT) [44] proves the role of closed or nearly closed shell effects, emerging from the cold reaction valley which corresponds to the potential energy minima in the calculated driving potential. The driving potential is defined as the difference between the interaction potential V and the decay energy Q of the reaction. The Q values are calculated using the mass tables of Wang *et al* [39] and for isotopes for which the values are not available, we have taken the values from the mass tables of Moller *et al* [40]. The driving potential ($V-Q$) for the parent nucleus is calculated for all possible fragments as a function of mass and charge asymmetries respectively given as

$$\eta = \frac{A_1 - A_2}{A_1 + A_2} \quad \text{and} \quad \eta_Z = \frac{Z_1 - Z_2}{Z_1 + Z_2},$$

at the touching configuration. For every fixed mass pair (A_1, A_2), a pair of charges is singled out for which the driving potential is minimised.

For a given mass of the middle fragment, say $A_2 = 34$, there are 11 possible Z_2 values ranging from 10 (^{34}Ne) to 20 (^{34}Ca). We have studied the fragmentation of ^{236}U isotope, keeping the middle fragment as ^{34}Ne, ^{34}Na, ^{34}Mg, ^{34}Al, ^{34}Si, ^{34}P, ^{34}S, ^{34}Cl, ^{34}Ar, ^{34}K and ^{34}Ca using the concept of cold reaction valley. Keeping the middle fragment as ^{34}Ca, the driving potential is calculated and plotted as a function of fragment mass number A_1 as shown in figure 2. It can be seen that with ^{34}Ca as the middle fragment, the combination ^{76}Ni+^{34}Ca+^{126}Ru has the least driving potential and high Q value. In the case of ^{34}Ne, ^{34}Na, ^{34}Mg and ^{34}Al as the middle fragments, fragment combinations with least driving potential and high Q value are found for ^{84}Se+^{34}Ne+^{118}Cd, ^{76}Ga+^{34}Na+^{126}Sn, ^{68}Ni+^{34}Mg+^{134}Te and ^{69}Ni+^{34}Al+^{133}Sb splittings, respectively. With ^{34}Si and ^{34}P as the middle fragments formed in the tripartition, fragment combinations with least driving potential and high Q value are found for ^{70}Ni + ^{34}Si + ^{132}Sn and ^{70}Co + ^{34}P + ^{132}Sn respectively. For $A_2 = 34$, other favourable fragment combinations found are for ^{70}Fe + ^{34}S + ^{132}Sn, ^{74}Ni + ^{34}Cl + ^{128}Ag, ^{76}Ni + ^{34}Ar + ^{126}Pd and ^{75}Ni + ^{34}K + ^{127}Rh, respectively in the case of middle fragments ^{34}S, ^{34}Cl, ^{34}Ar and ^{34}K. Among all the possible Z_2 values for $A_2 = 34$, the lowest driving potential is found for the fragment combination with ^{34}Si as the middle fragment. Thus, we can say that among all the possible charges for a particular mass number of the middle fragment $A_2 = 34$, the most favourable fragment combination is obtained for ^{70}Ni + ^{34}Si + ^{132}Sn, in the ternary fission of ^{236}U isotope in collinear configuration.

In order to prove our justification about the most favourable fragment combination, the barrier penetrability and hence the relative yield is calculated for the mass number of the middle fragment $A_2 = 34$ with charge ranging from $Z_2 = 10$ to 20. In the case of the middle fragment as ^{34}Ne, the barrier penetrability is

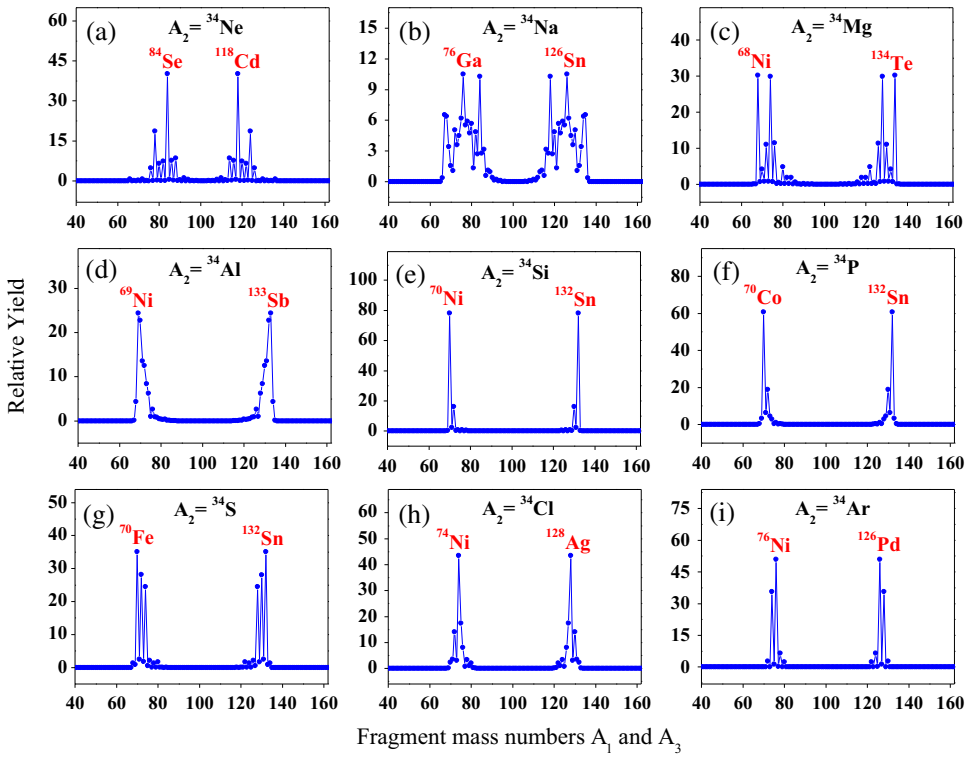

Figure 3. The relative yield plotted as a function of fragment mass numbers A_1 and A_3 for all possible middle fragments with mass number $A_2 = 34$.

calculated for all possible fragmentations found in the cold reaction valley and hence the relative yield is calculated and plotted as a function of fragment mass numbers A_1 and A_3 as shown in figure 3a. From figure 3a, it is clear that the highest relative yield is found for the fragment splitting ^{84}Se $+^{34}$Ne $+^{118}$Cd, which is the same fragment combination obtained with the least driving potential and high Q value from the cold reaction valley plot. For ^{34}Na and ^{34}Mg as the middle fragments, the highest relative yields are obtained for the fragment combinations ^{76}Ga $+^{34}$Mg $+^{126}$Sn and ^{68}Ni $+^{34}$Mg $+^{134}$Te respectively, whereas in the case of ^{34}Al and ^{34}Si, the highest relative yields are found for ^{69}Ni $+^{34}$Al $+^{133}$Sb and ^{70}Ni $+^{34}$Si $+^{132}$Sn respectively. In the case of middle fragments ^{34}P, ^{34}S, ^{34}Cl and ^{34}Ar, the highest relative yields are found for ^{70}Co$+^{34}$P$+^{132}$Sn, ^{70}Fe$+^{34}$S$+^{132}$Sn, ^{74}Ni$+^{34}$Cl$+^{128}$Ag and ^{76}Ni $+^{34}$Ar $+^{126}$Pd respectively. In a similar manner, the barrier penetrability and hence the relative yield is calculated for other possible fragmentations found for the particular mass number of the middle fragment $A_2 = 34$. Figure 3 represents the relative yield plotted as a function of fragment mass numbers A_1 and A_3, keeping the mass of the middle fragment as $A_2 = 34$. From figure 3, it can be seen that the highest magnitude of relative yield is found for the fragment combination ^{70}Ni$+^{34}$Si$+^{132}$Sn which includes the presence of doubly magic ^{132}Sn ($Z = 50$, $N = 82$) nuclei and the proton shell closure $Z = 28$ of ^{70}Ni. Here, we would like to mention that, the fragment combination obtained with highest relative yield for a particular mass $A_2 = 34$, is the same as that obtained with least driving potential and high Q value from the cold reaction valley plot. The fragment combination with the highest yield (minimum driving potential and maximum yield) for the tripartition of ^{236}U with $A_2 = 40, 46, 54, 56, 58$ are for ^{64}Fe$+$ ^{40}S $+^{132}$Sn, ^{58}Cr $+^{46}$Ar $+^{132}$Sn, ^{48}Ca $+^{54}$Ca $+^{134}$Te, ^{48}Ca $+^{56}$Ti $+^{132}$Sn, ^{48}Ca $+^{58}$Ti $+^{130}$Sn, respectively.

In a similar manner, the driving potential and the relative yield are calculated for all possible fragment combinations found in the tripartition of ^{236}U isotope. It should be noted that, about seven hundred thousand fragment splittings are possible in the tripartition of ^{236}U isotope, out of which the most favourable fragment combination for a particular mass number of the middle fragment ranges from $A_2 = 1$ to 78 is shortlisted. In figure 4, the driving potential of the most favourable fragment combination for a particular mass number of the middle fragment ranging from $A_2 = 1$ to 78 is plotted as a function of fragment mass number A_2 obtained in the tripartition of ^{236}U isotope.

Comparison of individual yield of the most favourable fragment combination for a particular mass number of the middle fragment ranging from $A_2 = 1$ to 78 is

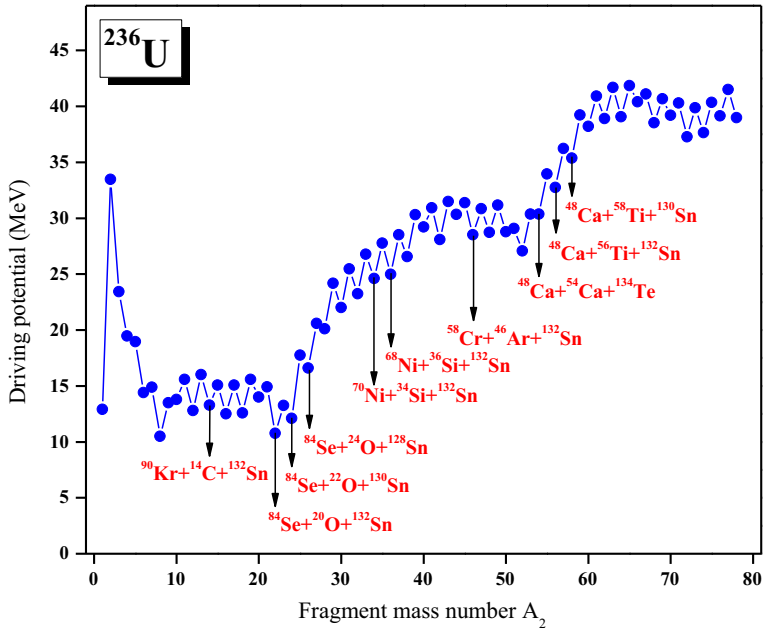

Figure 4. The driving potential of the most favourable fragment combination for a particular mass number of the middle fragment ranging from $A_2 = 1$ to 78 plotted as a function of fragment mass number A_2, in the tripartition of ^{236}U isotope.

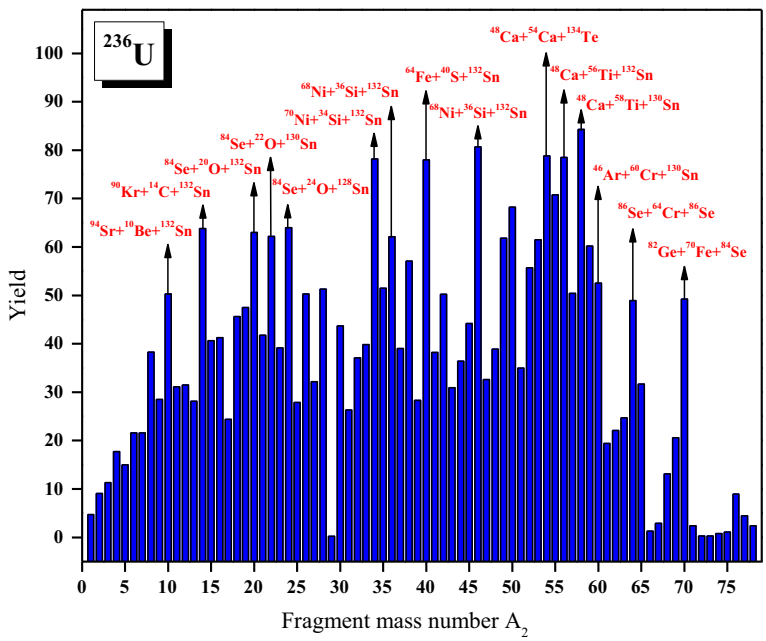

Figure 5. The yield of the most favourable fragment combination for a particular mass number of the middle fragment ranging from $A_2 = 1$ to 78, plotted as a function of fragment mass number A_2 in the tripartition of ^{236}U isotope.

plotted in figure 5 as a function of fragment mass number A_2. The fragment combinations with the yield greater than 60 obtained in the tripartition of ^{236}U are listed in table 1. The highest yield is obtained for the fragment combination ^{48}Ca+^{58}Ti+^{130}Sn, where ^{130}Sn ($Z = 50$, $N = 80$) is a near doubly magic nucleus and ^{48}Ca ($Z = 20$, $N = 28$) is a doubly magic nucleus. The next highest yield is obtained for the fragment combination ^{58}Cr+^{46}Ar+^{132}Sn, where ^{132}Sn ($Z = 50$, $N = 82$) is a doubly magic nucleus. The highest yield found for the fragment combinations ^{48}Ca+^{54}Ca+^{134}Te and ^{48}Ca+^{56}Ti+^{132}Sn is due to the presence of near doubly magic nucleus ^{134}Te ($Z = 52$, $N = 82$) and doubly magic nucleus ^{132}Sn ($Z = 50$, $N = 82$) respectively. It

Table 1. The fragment combinations obtained in the collinear tripartition of ^{236}U isotope with yield greater than 60.

First fragment A_1	Middle fragment A_2	Third fragment A_3	Q value (MeV)	Yield Y (%)
^{90}Kr	^{14}C	^{132}Sn	190.93	63.81
^{84}Se	^{20}O	^{132}Sn	191.14	62.98
^{84}Se	^{22}O	^{130}Sn	189.25	62.21
^{84}Se	^{24}O	^{128}Sn	183.26	63.97
^{70}Ni	^{34}Si	^{132}Sn	198.16	78.24
^{68}Ni	^{36}Si	^{132}Sn	194.84	62.18
^{64}Fe	^{40}S	^{132}Sn	196.80	78.07
^{58}Cr	^{46}Ar	^{132}Sn	200.55	80.72
^{54}Ti	^{49}K	^{133}Sb	196.58	61.83
^{52}Ca	^{50}Ca	^{134}Te	198.83	68.29
^{49}Ca	^{53}Ca	^{134}Te	194.74	61.50
^{48}Ca	^{54}Ca	^{134}Te	193.99	78.86
^{49}Ca	^{55}Ti	^{132}Sn	201.96	70.82
^{48}Ca	^{56}Ti	^{132}Sn	202.43	78.51
^{48}Ca	^{58}Ti	^{130}Sn	197.91	84.35
^{47}K	^{59}V	^{130}Sn	196.12	60.28

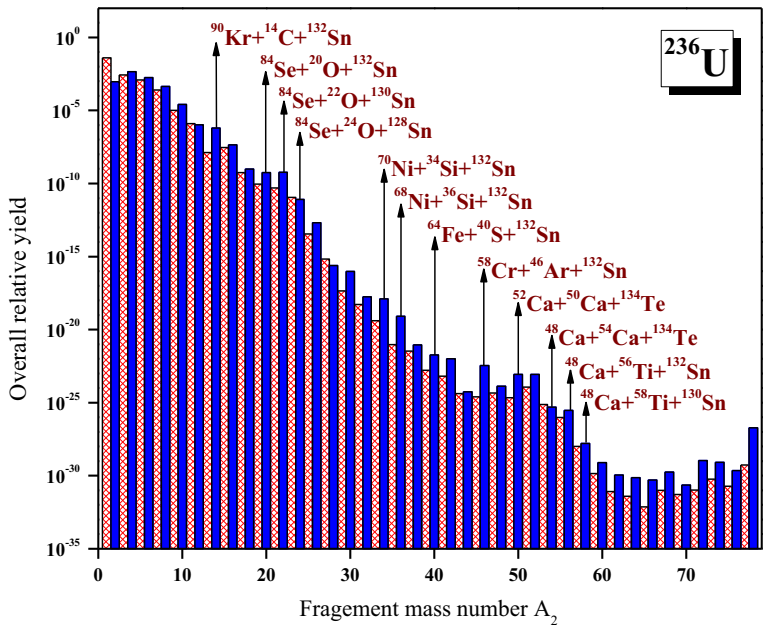

Figure 6. The overall relative yield of the most favourable fragment combination for a particular mass number of the middle fragment ranging from $A_2 = 1$ to 78, plotted as a function of fragment mass number A_2. Some of the fragment combinations ($A_1 + A_2 + A_3$) that are found in the tripartition of ^{236}U isotope are labelled.

should be noted that, in both cases the lighter fragment ^{48}Ca ($Z = 20$, $N = 28$) is a doubly magic nucleus. When ^{34}Si is the middle fragment, the highest yield is found for the fragment combination with ^{70}Ni (Z=28) and doubly magic nucleus ^{132}Sn ($Z = 50$, $N = 82$) as the edge fragments. When ^{36}Si is the middle fragment, the highest yield is found for the fragment combination with ^{68}Ni ($Z = 28$) and doubly magic nucleus ^{132}Sn ($Z = 50$, $N = 82$) as the edge fragments. Thus, the possibility for the formation of ^{68}Ni and ^{70}Ni as the edge fragments connecting the Sn isotope by Si, is proved in the tripartition of ^{236}U isotope using the unified ternary fission model. This observation is in good agreement with the result obtained from the theoretical analysis done by Nasirov *et al* [28] and Oertzen and Nasirov [30]. The formation of ^{68}Ni and ^{70}Ni as the

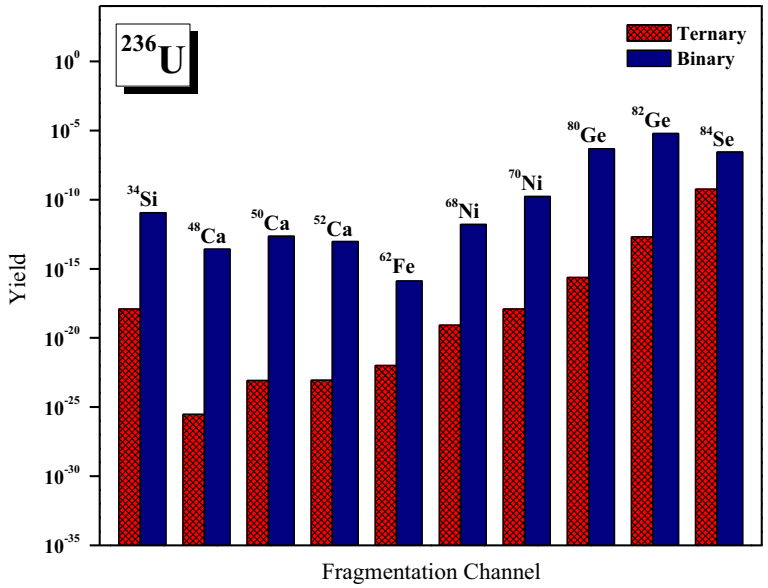

Figure 7. Comparison of yield of the favourable fragments obtained in the tripartition of ^{236}U with the binary fission of ^{236}U.

edge fragments connecting the ^{132}Sn isotope by Si, in the tripartition of ^{236}U observed in FOBOS experimental set-up by Pyatkov *et al* [23] proves the reliability of this work using unified ternary fission model.

An overall relative yield is calculated which is defined as the ratio of the penetration probability of a particular fragment to all the possible fragmentations with various fragment mass numbers A_2. The overall relative yield of the most favourable fragment combination for a particular mass number of the middle fragment ranging from $A_2 = 1$ to 78 is plotted in figure 6 as a function of fragment mass number A_2 in the tripartition of ^{236}U isotope.

In figure 7, the yield of the favourable fragments obtained in the tripartition of ^{236}U isotope is compared with the binary fission of ^{236}U isotope. It is clear from the graph that the yield obtained for the binary fission of ^{236}U isotope is higher than the tripartition of ^{236}U isotope.

4. Summary

The tripartition of ^{236}U isotope has been studied for all possible fragmentations using the recently proposed UTFM. The highest yield is found for the fragmentation ^{48}Ca+^{58}Ti+^{130}Sn, which possesses the doubly magic nucleus ^{48}Ca ($Z = 20$, $N = 28$) and near doubly magic nucleus ^{130}Sn ($Z = 50$, $N = 80$). The next highest yield is found for the fragmentation ^{58}Cr+^{46}Ar+^{132}Sn, which also possesses the doubly magic nucleus ^{132}Sn ($Z = 50$, $N = 82$). The presence of closed shell or doubly closed shell effect plays an important role in the tripartition of ^{236}U isotope. The formation of experimentally observed Ni isotope as the edge fragment connecting Sn isotope to Si has been theoretically proved in the tripartition of ^{236}U isotope using UTFM. The formation of ^{68}Ni and ^{70}Ni as the edge fragments linking the doubly magic nucleus ^{132}Sn and the isotope of Si is in good agreement with experimental [21] and theoretical studies [26,28] in the collinear cluster tripartition of ^{236}U isotope which reveals the reliability of our UTFM in ternary fission.

Acknowledgements

The author KPS would like to thank the University Grants Commission, Govt. of India for the financial support under Major Research Project No. 42-760/2013 (SR) dated 22-03-2013.

References

[1] R D Present, *Phys. Rev.* **59**, 466 (1941)
[2] L W Alvarez, as reported by G Farwell, E Segre and C Wiegand, *Phys. Rev.* **71**, 327 (1947)
[3] J F Wild, P A Baisden, R J Dougan, E K Hulet, R W Lougheed and J H Landrum, *Phys. Rev. C* **32**, 488 (1985)
[4] G Royer, F Haddad and J Mignen, *J. Phys. G: Nucl. Part. Phys.* **18**, 2015 (1992)
[5] D N Poenaru, B Dobrescu, W Greiner, J H Hamilton and A V Ramayya, *J. Phys. G: Nucl. Part. Phys.* **26**, L97 (2000)
[6] D M Nadkarni, *Nucl. Phys. A* **112**, 241 (1968)

[7] A V Ramayya *et al*, *Phys. Rev. C* **57**, 2370 (1998)
[8] S Vermote, C Wagemans, O Serot, J Heyse, J Van Gils, T Soldner, P Geltenbort, I Al Mahamid, G Tian and L Rao, *Nucl. Phys. A* **837**, 176 (2010)
[9] L Rosen and A M Hudson, *Phys. Rev.* **78**, 533 (1950)
[10] D N Poenaru, W Greiner and R A Gherghescu, *At. Data Nucl. Data Tables* **68**, 91 (1998)
[11] D N Poenaru, R A Gherghescu, W Greiner, Y Nagame, J H Hamilton and A V Ramayya, *Rom. Rep. Phys.* **55**, 549 (2003)
[12] V I Zagrebaev, A V Karpov and W Greiner, *Phys. Rev. C* **81**, 044608 (2010)
[13] K R Vijayaraghavan, M Balasubramaniam and W von Oertzen, *Phys. Rev. C* **90**, 024601 (2014)
[14] K R Vijayaraghavan, M Balasubramaniam and W von Oertzen, *Phys. Rev. C* **91**, 044614 (2015)
[15] K R Vijayaraghavan, W von Oertzen and M Balasubramaniam, *Eur. Phys. J. A* **48**, 27 (2012)
[16] K Manimaran and M Balasubramaniam, *Phys. Rev. C* **79**, 024610 (2009)
[17] K Manimaran and M Balasubramaniam, *Eur. Phys. J. A* **45**, 293 (2010)
[18] K Manimaran and M Balasubramaniam, *J. Phys. G: Nucl. Part. Phys.* **37**, 045104 (2010)
[19] K Manimaran and M Balasubramaniam, *Phys. Rev. C* **83**, 034609 (2011)
[20] M Balasubramaniam, K R Vijayaraghavan and C Karthikraj, *Pramana – J. Phys.* **85**, 423 (2015)
[21] R B Tashkhodjaev, A I Muminov, A K Nasirov, W von Oertzen and Yongseok Oh, *Phys. Rev. C* **91**, 054612 (2015)
[22] Yu V Pyatkov *et al*, *Phys. At. Nucl.* **66**, 1631 (2003)
[23] Yu V Pyatkov *et al*, *Phys. At. Nucl.* **73**, 1309 (2010)
[24] Yu V Pyatkov *et al*, *Eur. Phys. J. A* **45**, 29 (2010)
[25] Yu V Pyatkov *et al*, *Int. J. Mod. Phys. E* **20**, 1008 (2011)
[26] Yu V Pyatkov *et al*, *Eur. Phys. J. A* **48**, 94 (2012)
[27] Yu V Pyatkov *et al*, *Phys. At. Nucl.* **77**, 1518 (2014)
[28] A K Nasirov, W von Oertzen, A I Muminov and R B Tashkhodjaev, *Phys. Scr.* **89**, 054022 (2014)
[29] A K Nasirov, W von Oertzen and R B Tashkhodjaev, *Pramana – J. Phys.* **85**, 367 (2015)
[30] W von Oertzen and A K Nasirov, *Phys. Lett. B* **734**, 234 (2014)
[31] W von Oertzen, Y V Pyatkov and D Kamanin, *Acta Phys. Polon. B* **44**, 447 (2013)
[32] W von Oertzen, A K Nasirov and R B Tashkhodjaev, *Phys. Lett. B* **746**, 223 (2015)
[33] K P Santhosh, Sreejith Krishnan and B Priyanka, *Eur. Phys. J. A* **50**, 66 (2014)
[34] K P Santhosh, Sreejith Krishnan and B Priyanka, *J. Phys. G: Nucl. Part. Phys.* **41**, 105108 (2014)
[35] K P Santhosh, Sreejith Krishnan and B Priyanka, *Int. J. Mod. Phys. E* **23**, 1450071 (2014)
[36] K P Santhosh, Sreejith Krishnan and B Priyanka, *Int. J Mod. Phys. E* **24**, 1550001 (2015)
[37] K P Santhosh, Sreejith Krishnan and B Priyanka, *Phys. Rev. C* **91**, 044603 (2015)
[38] K P Santhosh and Sreejith Krishnan, *Eur. Phys. J. A* **52**, 108 (2016)
[39] M Wang, G Audi, A H Wapstra, F G Kondev, M Mac Cormick, X Xu and B Pfeiffer, *Chin. Phys. C* **36**, 1603 (2012)
[40] P Moller, A J Sierk, T Ichikawa, H Sagawa, *At. Data Nucl. Data Tables* **109**, 1 (2016)
[41] J Blocki, J Randrup, W J Swiatecki and C F Tsang, *Ann. Phys. (N.Y.)* **105**, 427 (1977)
[42] J Blocki and W J Swiatecki, *Ann. Phys. (N.Y.)* **132**, 53 (1983)
[43] W D Myers and W J Swiatecki, *Ark. Fys.* **36**, 343 (1967)
[44] R K Gupta, in *Heavy elements and related new phenomena* edited by R K Gupta and W Greiner (World Scientific, Singapore, 1999) Vol. II, p. 730